AIR FORCE REPORT NO.
SAMSO-TR-72-176

AEROSPACE REPORT NO.
TR-0172(2240-30)-5

AD 745962

Response of a Curved Elastic Segment to Shock Wave Engulfment Loads

Prepared by J. P. JONES and S. OKUBO
Aerodynamics and Propulsion Research Laboratory

72 JUN 30

D D C
RECEIVED
AUG 1 1972
B

Laboratory Operations
THE AEROSPACE CORPORATION

Prepared for SPACE AND MISSILE SYSTEMS ORGANIZATION
AIR FORCE SYSTEMS COMMAND
LOS ANGELES AIR FORCE STATION
Los Angeles, California

NATIONAL TECHNICAL
INFORMATION SERVICE

DISTRIBUTION STATEMENT A
APPROVED FOR PUBLIC RELEASE.
DISTRIBUTION UNLIMITED

LABORATORY OPERATIONS

The Laboratory Operations of The Aerospace Corporation is conducting experimental and theoretical investigations necessary for the evaluation and application of scientific advances to new military concepts and systems. Versatility and flexibility have been developed to a high degree by the laboratory personnel in dealing with the many problems encountered in the nation's rapidly developing space and missile systems. Expertise in the latest scientific developments is vital to the accomplishment of tasks related to these problems. The laboratories that contribute to this research are:

Aerodynamics and Propulsion Research Laboratory: Launch and reentry aerodynamics, heat transfer, reentry physics, propulsion, high-temperature chemistry and chemical kinetics, structural mechanics, flight dynamics, atmospheric pollution, and high-power gas lasers.

Electronics Research Laboratory: Generation, transmission, detection, and processing of electromagnetic radiation in the terrestrial and space environments, with emphasis on the millimeter-wave, infrared, and visible portions of the spectrum; design and fabrication of antennas, complex optical systems and photolithographic solid-state devices; test and development of practical superconducting detectors and laser devices and technology, including high-power lasers, atmospheric pollution, and biomedical problems.

Materials Sciences Laboratory: Development of new materials; metal matrix composites and new forms of carbon; test and evaluation of graphite and ceramics in reentry, spacecraft materials and components in radiation and high-vacuum environments; application of fracture mechanics to stress corrosion and fatigue-induced fractures in structural metals; effect of nature of material surfaces on lubrication, photosensitization, and catalytic reactions, and development of prosthesis devices.

Plasma Research Laboratory: Reentry physics and nuclear weapons effects; the interaction of antennas with reentry plasma sheaths, experimentation with thermonuclear plasmas; the generation and propagation of plasma waves in the magnetosphere; chemical reactions of vibrationally excited species in rocket plumes, and high-precision laser ranging.

Space Physics Laboratory: Aeronomy, density and composition of the atmosphere at all altitudes; atmospheric reactions and atmospheric optics; pollution of the environment; the sun, earth's resources, meteorological measurements; radiation belts and cosmic rays, and the effects of nuclear explosions, magnetic storms, and solar radiation on the atmosphere.

THE AEROSPACE CORPORATION
El Segundo, California

ACCESSION for
NTIS White Section ☑
DDC Buff Section ☐
UNANNOUNCED ☐
JUSTIFICATION
BY
DISTRIBUTION/AVAILABILITY CODES
Dist. AVAIL. and/or SPECIAL
A

UNCLASSIFIED
Security Classification

DOCUMENT CONTROL DATA - R & D

(Security classification of title, body of abstract and indexing annotation must be entered when the overall report is classified)

1. ORIGINATING ACTIVITY *(Corporate author)* The Aerospace Corporation El Segundo, California	2a REPORT SECURITY CLASSIFICATION Unclassified 2b GROUP

3. REPORT TITLE

RESPONSE OF A CURVED ELASTIC SEGMENT TO SHOCK-WAVE ENGULFMENT LOADS

4. DESCRIPTIVE NOTES *(Type of report and inclusive dates)*

5. AUTHOR(S) *(First name, middle initial, last name)*

John Paul Jones and Seichi Okubo

6. REPORT DATE 72 JUN 30	7a TOTAL NO. OF PAGES 30	7b. NO. OF REFS 10
8a CONTRACT OR GRANT NO. F04701-71-C-0172 b PROJECT NO. c d	9a ORIGINATOR'S REPORT NUMBER(S) TR-0172(2240-30)-5 9b OTHER REPORT NO(S) *(Any other numbers that may be assigned this report)* SAMSO-TR-72-176	

10. DISTRIBUTION STATEMENT

Approved for public release; distribution unlimited

11. SUPPLEMENTARY NOTES	12. SPONSORING MILITARY ACTIVITY Space and Missile Systems Organization Air Force Systems Command Los Angeles, California

13. ABSTRACT

The short time response of a cylindrical, elastic segment to shock-wave engulfment is treated. The exact equations of the linear theory of elasticity are used instead of the usual integrated equations of ring theory. Using a relatively new mathematical technique, described in the report, we easily identify the focusing effects due to the curved geometry. This work explains some anomalous results obtained while subjecting curved aluminum specimens to loads produced by shock waves.

DD FORM 1473

UNCLASSIFIED
Security Classification

14. KEY WORDS

Composite materials
Elasto dynamics
Ring engulfment
Short-time composite materials

Distribution Statement (Continued)

Abstract (Continued)

Air Force Report No.
SAMSO-TR-72-176

Aerospace Report No.
TR-0172(2240-30)-5

RESPONSE OF A CURVED ELASTIC SEGMENT TO SHOCK-WAVE ENGULFMENT LOADS

Prepared by

J. P. Jones and S. Okubo
Aerodynamics and Propulsion Research Laboratory

72 JUN 30

Laboratory Operations
THE AEROSPACE CORPORATION

Prepared for

SPACE AND MISSILE SYSTEMS ORGANIZATION
AIR FORCE SYSTEMS COMMAND
LOS ANGELES AIR FORCE STATION
Los Angeles, California

Approved for public release;
distribution unlimited

FOREWORD

This report is published by The Aerospace Corporation, El Segundo, California, under Air Force Contract No. F04701-71-C-0172.

This report, which documents research carried out from 1 July 1971 through 1 May 1972, was submitted on 19 May 1972 to Capt Gary R. Edwards, SYAE, for review and approval.

Acknowledgment is made of the many helpful discussions and the advice of Julius Miklowitz.

Approved

W. R. Warren, Director
Aerodynamics and Propulsion
Research Laboratory

Publication of this report does not constitute Air Force approval of the report's findings or conclusions. It is published only for the exchange and stimulation of ideas.

Gary R. Edwards, Capt, USAF
Project Officer

ABSTRACT

The short time response of a cylindrical, elastic segment to shock-wave engulfment is treated. The exact equations of the linear theory of elasticity are used instead of the usual integrated equations of ring theory. Using a relatively new mathematical technique, described in the report, we easily identify the focusing effects due to the curved geometry. This work explains some anomalous results obtained while subjecting curved aluminum specimens to loads produced by shock waves.

CONTENTS

FOREWORD ii

ABSTRACT iii

LIST OF SYMBOLS vii

I. INTRODUCTION 1

II. ANALYSIS 5

III. INVERSION 19

IV. NUMERICAL RESULTS AND CONCLUSIONS 25

REFERENCES 27

FIGURES

1. Flat Specimen Trace 2

2. Curved Specimen Trace 2

3. Ring Geometry 4

4. Multiple Reverberation Trace 23

Preceding page blank

LIST OF SYMBOLS

A, B, C, D	Integration constants
C_p, C_s	α, β
E	Young's modulus
$f(s, \nu)$	See equation (15).
$F_i(x)$, $G_i(x)$, $H_i(x)$	See pages 9 and 10.
$g(\nu, x)$	See equation (21).
$h(\nu, x)$	$(\nu^2 + x^2)^{1/4}$
k_1, k_2	See equation (42).
p_o	Applied pressure
r, t	$\hat{r}$, $\alpha\hat{t}/r_1$
r_1, r_0	Outer radius, inner radius
$\hat{r}$, θ, $\hat{t}$	Plane polar coordinates, time
t_p, t_s	$(r_1 - r_0)/c_p$, $(r_1 - r_o)/c_s$
U_1, U_2, V_1, V_2	See equation (23).
u, v	Radial displacement, tangential displacement
V, v	Load velocity, V/α
α, β, η	$[(\lambda + \nu\mu)/\rho]^{1/2}$, $(\mu/\rho)^{1/2}$, α/β
γ	r_0/r_1
ϵ, δ	See equation (24).

Preceding page blank

LIST OF SYMBOLS (Continued)

λ, μ	Lamé elastic parameters
ν, s	Fourier and Laplace transform variables
ρ, w	Density, specific weight
σ_r, $\sigma_{r\theta}$, etc.	Stress tensor components
ϕ, ψ	Dilatational potential, equivoluminar potential

I. INTRODUCTION

Recently, a facility was developed to measure the short time effects of the response of materials to a step-function pressure pulse [1]. This has proven efficacious in the measurement and prediction of the dispersive properties of materials [10]. Loading is applied to the specimen* by means of a shock tube and provides a clean step function of up to 70 psi with a rise time of less than 15 nsec. The back-face velocity of the specimen is measured by a capacitance gauge, and, in the usual case, the one-dimensional theories used are good for a few reverberations. A flat aluminum specimen is used for calibration since it is quite dispersion free. A typical oscilloscope trace of the back-face velocity is shown in Fig. 1.

In order to extend this technique to geometries other than flat specimens, recently, some cylindrical segments were tested. The results for an aluminum specimen (Fig. 2) show, instead of the usual "staircase" response (Fig. 1), a jump followed by a rise and then a downward slope. It was easily ascertained that this phenomenon was not due to malfunctions of the test apparatus. Thus, this effect must come from the curved geometry.

It is the purpose of this work to explain these phenomena. Two major assumptions were used in order to simplify the problem. The first was to idealize the ring segment to that of a full ring. This was a valid approximation since only short times were of interest, and the experiment was normally

*Although the specimen can vary in size, the usual sample is a flat specimen 1.25 in. × 1.25 in. × 0.25 in.

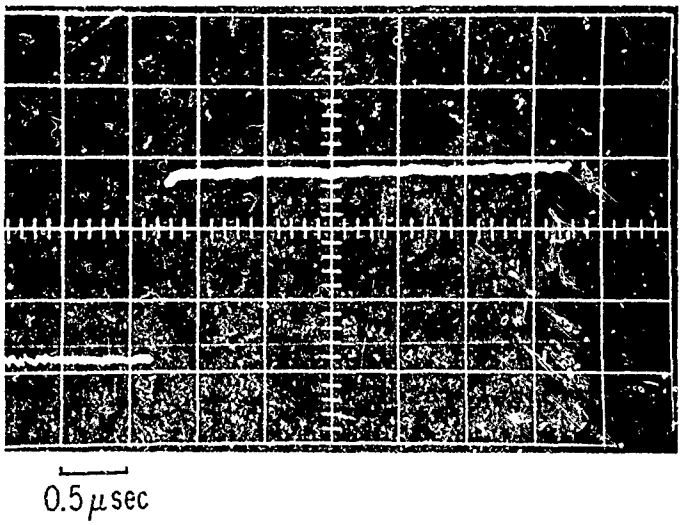

Fig. 1. Flat Specimen Trace

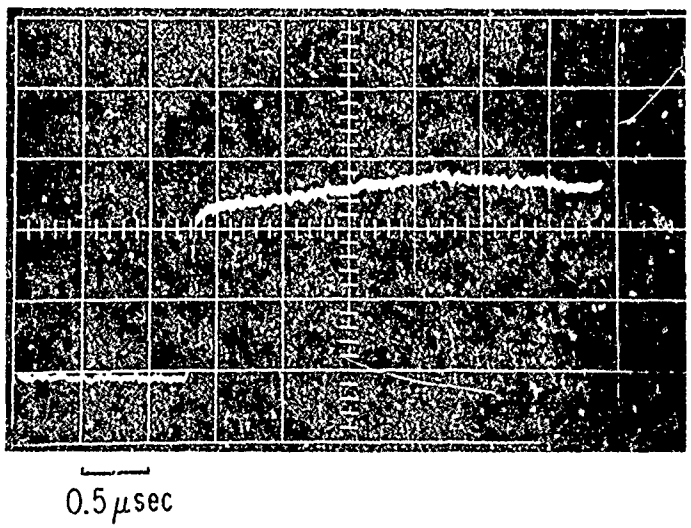

Fig. 2. Curved Specimen Trace

considered finished when effects from the boundaries of the specimen arrived at the point where the back-face velocity was measured, in this case, at $\theta = 0$ (Fig. 3). The second assumption was that the effects of shock diffraction were negligible, and that the shock wave acted as a pressure pulse, unchanged in pressure as it engulfed the specimen. This assumption was made on the basis of preliminary calculations and the fact that the theory compared well with experiments.

The results of the present analysis show that the first ramp is due to successive P wave arrivals as the engulfment ensued and to the focusing effects of curved media. The downward ramp is shown to be due to S wave arrivals. Rather than the usual modal approach, we proceed with the technique used by Friedlander [4], in which the solution is taken as a wave sum, each term of which is identified with one sheet of an infinite-sheeted Riemann surface over the propagation coordinate (circumferential θ here).

The problem of the engulfment of a ring has been treated by several authors of which Bleich and Mindlin [2] and Payton [3] are the most germane to the present work. These authors are primarily interested in the structural response of a ring rather than the wave propagation through the thickness as in the present work. The equations of the linear theory of elasticity are the equations pertinent to the present problem and not the integrated ring equations used in references [2] and [3].

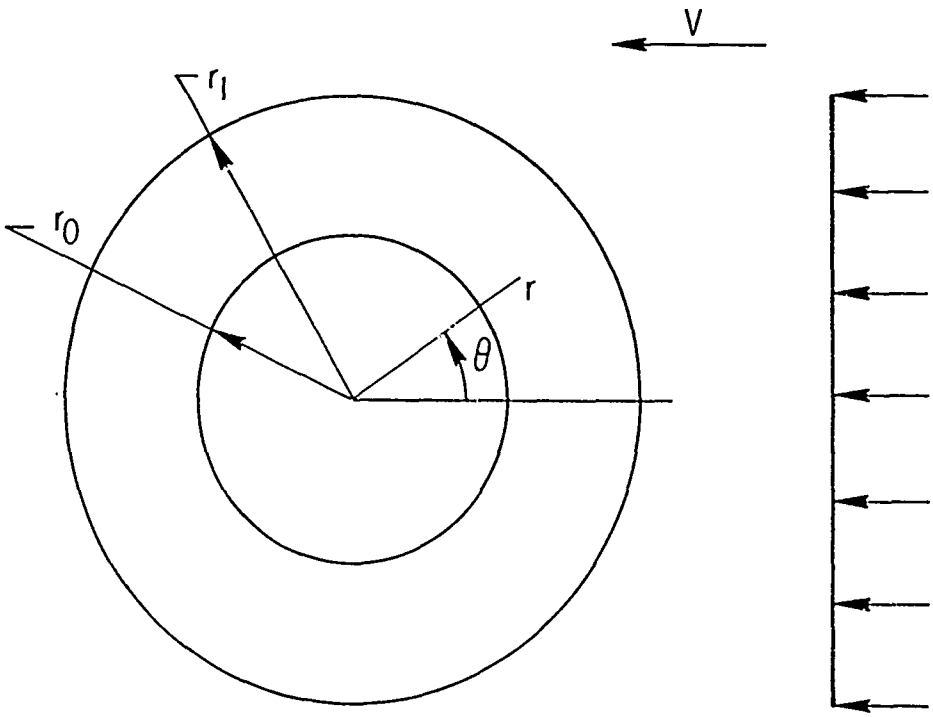

Fig. 3. Ring Geometry

II. ANALYSIS

As was mentioned in the Introduction, a cylindrical specimen is hit by a shock wave that is, to a close approximation, a step-function pressure input. The problem considered in the present work is the calculation of the velocity of the back surface directly behind the specimen at $\theta = 0$. The times of interest are those necessary for the first few reverberations. Accordingly, a solution valid for small times is sought.

Consider an elastic ring of inner radius r_0 and outer radius r_1. It has a flat pressure pulse of strength p_o impinging on it with velocity V (Fig. 3). The elastic parameters are λ, μ, and ρ, and the problem is treated as that of plane strain. Time is denoted by $\hat{t}$, and polar coordinates by $\hat{r}$ and θ. Setting

$$r = \frac{\hat{r}}{r_1} \qquad t = \frac{\alpha \hat{t}}{r_1} \qquad \eta = \frac{\alpha}{\beta} \tag{1}$$

where α and β are the dilatational and equivoluminal speeds given by $\alpha^2 = (\lambda + 2\mu)/\rho$ and $\beta^2 = \mu/\rho$, respectively, one gets the equations of elastodynamics

$$\nabla^2 \phi = \phi,_{tt} \qquad \nabla^2 \psi = \eta^2 \psi,_{tt} \tag{2}$$

$$r_1 u = \phi,_r + r^{-1} \psi,_\theta \qquad r_1 v = r^{-1} \phi,_\theta - \psi,_r \tag{3}$$

$$\frac{r_1^2\sigma_r}{\mu} = (\eta^2 - 2)\nabla^2\phi + 2\left(\phi,_{rr} + r^{-1}\psi,_{r\theta} - r^{-2}\psi,_{\theta}\right)$$

$$\frac{r_1^2\sigma_{r\theta}}{\mu} = 2\left(r^{-1}\phi,_{r\theta} - \phi,_{\theta}\right) - \psi,_{rr} + r^{-1}\psi,_{r} + r^{-2}\psi,_{\theta\theta}$$

$$\frac{r_1^2(\sigma_r + \sigma_\theta)}{\mu} = 2(\eta^2 - 1)\nabla^2\phi \tag{4}$$

where $\nabla^2 = \partial^2/\partial r^2 + r^{-1}\partial/\partial r + r^{-2}\partial/\partial\theta^2$, u and v are the radial and circumferential displacements, respectively, and σ_r, σ_θ, and $\sigma_{r\theta}$ are the usual stress components. The initial and boundary conditions are

$$\phi = \phi,_t = \psi = \psi,_t = 0 \qquad \gamma \le r \le 1 \qquad t = 0 \qquad \gamma = \frac{r_0}{r_1} \tag{5}$$

$$\sigma_r = -p_o H(vt - r\cos\theta) \qquad \sigma_{r\theta} = 0 \qquad r = 1 \qquad t > 0$$

$$\sigma_r = \sigma_{r\theta} = 0 \qquad r = \gamma \qquad t > 0 \tag{6}$$

where $v = V/\alpha$.

In theory, one can solve this problem by expanding all quantities in a Fourier series in θ, taking a Laplace transform in time, solving the resulting ordinary differential equation, and inverting the transform by residue theory. Such a process, however, is not well suited to short times or to discontinuous solutions [2]. A method that appears to be particularly well suited to problems of this type is that based on the work of Friedlander [4]. In this method,

solutions are sought of the form

$$\phi,\psi(r,\theta,t) = \sum_{n=-\infty}^{\infty} \phi^*,\psi^*(r,\theta + 2n\pi,t) \tag{7}$$

Instead of summing the "modes" of the solution, the form of equation (7) replaces the ring by a fictitious series of Riemann sheets spiralling over each other to provide an analytical continuation of θ to $\pm\infty$. Longer times mean that more Riemann sheets must be looked at. However, until the disturbance reaches $\theta = \pm\pi$, only the first sheet, $n = 0$, needs to be considered. In the present analysis, this is ideal, since only small times are of interest. Either of the preceding techniques, when carried to completion, yields the exact solution. The method of Friedlander is used here to provide the information desired in the easiest manner.

Supplanting the Fourier series by the successive infinite sets of Riemann sheets, we extend consideration of θ from $[-\pi, \pi]$ to $(-\infty, \infty)$. Accordingly, an exponential Fourier transform is indicated.* If $F(\theta)$ is a function and $\tilde{F}(\nu)$ its transform, then the pair can be defined as

$$\tilde{F}(\nu) = \int_{-\infty}^{\infty} F(\theta)\, e^{i\nu\theta}\, d\theta$$

$$F(\theta) = \frac{1}{2\pi} \int_{-\infty}^{\infty} \tilde{F}(\nu)\, e^{-i\nu\theta}\, d\nu \tag{8}$$

*For a more complete explanation of this method, see references [3] - [6].

Performing this operation, and at the same time taking a Laplace transform in time on equations (2)-(4), one has

$$\tilde{\bar{\phi}}_{,rr} + r^{-1}\tilde{\bar{\phi}}_{,r} - (\nu^2 r^{-2} + s^2)\tilde{\bar{\phi}} = 0$$

$$\tilde{\bar{\psi}}_{,rr} + r^{-1}\tilde{\bar{\psi}}_{,r} - (\nu^2 r^{-2} + \eta^2 s^2)\tilde{\bar{\psi}} = 0 \tag{9}$$

$$r_1\tilde{\bar{u}} = \tilde{\bar{\phi}}_{,r} - i\nu r^{-1}\tilde{\bar{\psi}}$$

$$r_1\tilde{\bar{v}} = -i\nu r^{-1}\tilde{\bar{\phi}} - \tilde{\bar{\psi}}_{,r} \tag{10}$$

$$r_1^2\frac{\tilde{\bar{\sigma}}_r}{\mu} = \left(\eta^2 s^2 + 2\frac{\nu^2}{r^2}\right)\tilde{\bar{\phi}} - 2\frac{\tilde{\bar{\phi}}_{,r}}{r} + 2i\nu\left(\frac{\tilde{\bar{\psi}}}{r^2} - \frac{\tilde{\bar{\psi}}_{,r}}{r}\right)$$

$$r_1^2\frac{\sigma_{r\theta}}{\mu} = 2i\nu\left(\frac{\tilde{\bar{\phi}}}{r^2} - \frac{\tilde{\bar{\phi}}_{,r}}{r}\right) - \left(\eta^2 s^2 + \frac{2\nu^2}{r^2}\right)\tilde{\bar{\psi}} + 2\frac{\tilde{\bar{\psi}}_{,r}}{r}$$

$$r_1^2\frac{(\sigma_r + \sigma_\theta)}{\mu} = 2(\eta^2 - 1)s^2\tilde{\bar{\phi}} \tag{11}$$

In equations (9)-(11), s denotes the Laplace transform variable and a bar denotes a Laplace transform.

The solution to equation (9) is

$$\tilde{\bar{\phi}} = AI_\nu(sr) + BK_\nu(sr)$$

$$\tilde{\bar{\psi}} = CI_\nu(\eta sr) + DK_\nu(\eta sr) \tag{12}$$

where I_ν and K_ν are modified functions of the first and second kinds, and A, B, C, and D are constants of integration. Equations (10) and (11) yield

$$r_1\tilde{\bar{u}} = s\left[AI_\nu'(sr) + BK_\nu'(sr)\right] - i\nu\eta s\left[C\frac{I_\nu(\eta sr)}{\eta sr} + D\frac{K_\nu(\eta sr)}{\eta sr}\right]$$

$$r_1\tilde{\bar{v}} = i\nu s\left[A\frac{I_\nu(sr)}{sr} + B\frac{K_\nu(sr)}{sr}\right] - \eta s\left[CI_\nu'(\eta sr) + DK_\nu'(\eta sr)\right]$$

$$r_1^2\frac{\tilde{\bar{\sigma}}r}{\mu} = s^2[AF_1(sr) + BK_2(sr)] + 2i\nu\eta^2 s^2[CG_1(\eta sr) + DG_2(\eta sr)]$$

$$r_1^2\frac{\tilde{\bar{\sigma}}r\theta}{\mu} = 2i\nu s^2[AG_1(sr) + BG_2(sr)] - \eta^2 s^2[CH_1(\eta sr) + DH_2(\eta sr)] \qquad (13)$$

where

$$F_1(x) = \left(\eta^2 + \frac{2\nu^2}{x^2}\right)I_\nu(x) - 2\frac{I_\nu'(x)}{x}$$

$$F_2(x) = \left(\eta^2 + \frac{2\nu^2}{x^2}\right)K_\nu(x) - 2\frac{K_\nu'(x)}{x}$$

$$G_1(x) = \frac{I_\nu(x)}{x^2} - \frac{I_\nu'(x)}{x}$$

$$G_2(x) = \frac{K_\nu(x)}{x^2} - \frac{K_\nu'(x)}{x}$$

$$H_1(x) = \left(1 + \frac{2\nu^2}{x^2}\right) I_\nu(x) - 2\frac{I_\nu(x)}{x}$$

$$H_2(x) = \left(1 + \frac{2\nu^2}{x^2}\right) K_\nu(x) - 2\frac{K_\nu(x)}{x} \qquad (14)$$

The boundary conditions, in general terms, are

$$\tilde{\bar{\sigma}}_r = -f(s,\nu) \qquad \tilde{\bar{\sigma}}_{r\theta} = 0 \qquad (\text{at } r = 1)$$

$$\tilde{\bar{\sigma}}_r = \tilde{\bar{\sigma}}_{r\theta} = 0 \qquad \left(\text{at } r = \gamma \equiv \frac{r_0}{r_1}\right) \qquad (15)$$

Thus, the boundary conditions yield

$$F_1(s)A + F_2(s)B + 2i\nu\eta^2[G_1(\eta s)C + G_2(\eta s)D] = \frac{-f(\nu, s)r_1^2}{\mu s^2}$$

$$2i\nu[G_1(s)A + G_2(s)B] - \eta^2[H_1(\eta s)C + H_2(\eta s)D] = 0$$

$$F_1(\gamma s)A + F_2(\gamma s)B + 2i\nu\eta^2[G_1(\eta\gamma s)C + G_2(\eta\gamma s)D] = 0$$

$$2i\nu[G_1(\gamma s)A + G_2(\gamma s)B] - \eta^2[H_1(\eta\gamma s)C + H_2(\eta\gamma s)D] = 0 \qquad (16)$$

Ideally, equation (13) can be solved for A, B, C, and D, and then explicit expressions can be obtained for the double transform of all pertinent quantities. These transforms then lead to the formal solution (inversion integrals) in the usual way. Since the present work deals only with short times and a different method is used, the resulting expressions are not given.

In order to apply this present method, the input or pressure function must be expanded in a series of the form given by equation (7). This can be done directly [6] by applying the Poisson summation formula

$$\sum_{n=-\infty}^{\infty} F(n) = \sum_{m=-\infty}^{\infty} \int_{-\infty}^{\infty} F(\nu)\, e^{2m\pi\nu i}\, d\nu \tag{17}$$

The applied stress at $r = 1$ is given by the first equation of equation (6). Thus,

$$\bar{\sigma}_r = \frac{-p_o}{s}\, e^{-(r/v)\cos\theta} \tag{18}$$

Following reference [6] and using equations (17) and (16), one gets

$$f(\nu, s) = \frac{2\pi p_o}{s}\, I_{|\nu|}\left(\frac{s}{v}\right) e^{-(s/v)} \tag{19}$$

It will be seen later that the absolute value sign on $I_{|\nu|}$ can be dropped.

If one applies the Laplace transform theory, the behavior of a function for small values of t is associated with large values of s [7]. However, for the present problem, in order to invert the Fourier transform, an integration with respect to ν must be made over the entire range $\nu \epsilon (-\infty, \infty)$. One is thus led to consider asymptotic expansions of I_ν and K_ν uniformly valid in ν for large values of s. Such asympotic expansions have been investigated by

Olver [8, 9] and are [10]:

$$I_\nu(x) \cong \frac{1}{\sqrt{2\pi}} \frac{e^{g(\nu,x)}}{h(\nu,x)}$$

$$K_\nu'(x) \cong \sqrt{\frac{\pi}{2}} \frac{e^{-g(\nu,x)}}{h(v,x)}$$

$$I_\nu'(x) \cong \frac{1}{\sqrt{2\pi}} \frac{h(\nu,x)}{x} e^{g(\nu,x)}$$

$$K_\nu'(x) \cong \sqrt{\frac{\pi}{2}} \frac{h(\nu,x)}{x} e^{-g(\nu,x)} \tag{20}$$

where

$$h(\nu,x) = (\nu^2 + x^2)^{1/4}$$

$$g(\nu,x) = \left(\nu^2 + x^2\right)^{1/2} - \nu \ln\left[\frac{\nu}{x} + \left(1 + \frac{\nu^2}{x^2}\right)^{1/2}\right] \tag{21}$$

These are uniformly valid in ν for $x \gg 1$. Since all quantities of interest always depend upon ν, the explicit notation for dependence is dropped for convenience. Thus, $h(\nu,x)$ and $g(\nu,x)$ are denoted by $h(x)$ and $g(x)$ in the following. Using equations (20) and (21) in the boundary conditions [equation (16)], for large s, one has

$$\frac{\eta^2}{h(s)} (U_1 \sinh \epsilon + V_1 \cosh \epsilon) - \frac{2i\nu}{\eta^2 s^2} h(\eta s) (U_2 \sinh \delta + V_2 \cosh \delta) = \frac{-f(\nu, s) r_1^2}{\mu s^2} \tag{22 (cont.)}$$

$$\frac{2i\nu}{s^2} h(s)(U_1 \cosh \epsilon + V_1 \sinh \epsilon) + \frac{\eta^2}{h(\eta s)} (U_2 \cosh \delta + V_2 \sinh \delta) = 0$$

$$\frac{\eta^2}{h(\gamma s)} V_1 - \frac{2i\nu}{\eta^2 \gamma^2 s^2} h(\eta\gamma s) V_2 = 0$$

$$\frac{2i\nu}{\gamma^2 s^4} h(\gamma s) U_1 + \frac{\eta^2}{h(\eta\gamma s)} U_2 = 0 \tag{22}$$

where, for convenience, one has set

$$U_1 = \frac{A}{\sqrt{2\pi}} e^{g(\gamma s)} - B\sqrt{\frac{\pi}{2}}\, e^{-g(\gamma s)} \qquad U_2 = \frac{C}{\sqrt{2\pi}} e^{g(\eta\gamma s)} + D\sqrt{\frac{\pi}{2}}\, e^{-g(\eta\gamma s)}$$

$$V_1 = \frac{A}{\sqrt{2\pi}} e^{g(\gamma s)} + B\sqrt{\frac{\pi}{2}}\, e^{-g(\gamma s)} \qquad V_2 = \frac{C}{\sqrt{2\pi}} e^{g(\eta\gamma s)} - D\sqrt{\frac{\pi}{2}}\, e^{-g(\eta\gamma s)} \tag{23}$$

and where

$$\epsilon = g(s) - g(\gamma s)$$

$$\delta = g(\eta s) - g(\eta\gamma s) \tag{24}$$

In order to assess magnitudes of terms, it is necessary for one to examine the properties of ϵ and δ before solving equation (22). It suffices for one to consider ϵ alone.

$$\epsilon(\nu, s) = (\nu^2 + s^2)^{1/2} - (\nu^2 + \gamma^2 s^2)^{1/2} - \nu \ln \gamma \frac{\nu + (\nu^2 + s^2)^{1/2}}{\nu + (\nu^2 + \gamma^2 s^2)^{1/2}} \tag{24.1}$$

It can easily be seen that

$$\epsilon(0, s) = s(1 - \gamma) > 0$$

$$\epsilon(\nu, s) \to -\nu \ln \gamma > 0 \qquad (\text{as } \nu \to \infty) \tag{24.2}$$

also

$$\frac{\partial \epsilon}{\partial \nu} = -\nu \ln \gamma \, \frac{\nu + (\nu^2 + s^2)^{1/2}}{\nu + (\nu^2 + \gamma^2 s^2)^{1/2}} > 0 \tag{24.3}$$

Thus, $\epsilon(\nu, s)$ is always positive and increases monotonically.

The solution of equation (22) is now routine. As $u_{,t}$ at the back face and at $\theta = 0$ is all that is required, only U_1 and U_2 will be solved for, since,

$$\frac{r_1 \tilde{\tilde{u}}}{s^2} = \frac{h(\gamma s)}{\gamma s} U_1 - \frac{i\nu}{\gamma s} \frac{1}{h(\eta\gamma s)} U_2 \tag{25}$$

Solving for U_1 and U_2, one gets

$$U_1 = -\frac{f(\nu, s) r_1^2}{\mu s^2 \Delta} \frac{\eta^2}{h(\eta\gamma s)} \left[\eta^4 \frac{\sinh \delta}{h(\gamma s) h(\gamma s)} - \frac{4\nu^2}{\eta^2 \gamma^2 s^4} h(s) h(\eta\gamma s) \sinh \epsilon \right]$$

$$U_2 = \frac{f(\nu, s) r_1^2}{\mu s^2 \Delta} \frac{2\nu}{\gamma^2 s^2} h(\gamma s) \left[\eta^4 \frac{\sinh \delta}{h(\gamma s) h(\eta s)} - \frac{4\nu^2}{\eta^2 \gamma^2 s^4} h(s) h(\eta\gamma s) \sinh \epsilon \right] \tag{26}$$

where Δ is the system determinant given by

$$\Delta = \frac{-\eta^8 \sinh \epsilon \sinh g}{h(s)h(\gamma s)h(\eta s)h(\eta\gamma s)} + \eta^4 \frac{4\nu^2}{s^4} \frac{h^2(s)h^2(\eta s) + \gamma^4 h^2(\gamma s)h^2(\eta\gamma s)}{h(s)h(\gamma s)h(\eta s)h(\eta\gamma s)}$$

$$\times \cosh \delta \cosh \epsilon + \frac{16\nu^4}{\gamma^4 s^8} h(s)h(\gamma s)h(\eta s)h(\eta\gamma s) \sinh \epsilon \sinh \delta$$

$$+ \frac{8\nu^2\eta^4}{\gamma^2 s^4} \tag{27}$$

The procedure now is to substitute equation (27) into equation (26), integrate on ν on an appropriate path to invert the θ transform and evaluate for large values of s. As it stands, this is difficult because of the form of Δ and h, and because the saddle path in the ν plane is not yet defined. In order to proceed, one recasts Δ into

$$\Delta = \frac{e^{\epsilon} e^{\delta} \eta^8}{4h(s)h(\gamma s)h(\eta s)h(\eta\gamma s)}$$

$$\times \left(- \left\{ 1 - \frac{\nu^2}{\eta^4 s^4} \left[h^2(s)h^2(\eta s) + \frac{h^2(\gamma s)h^2(\eta\gamma s)}{\gamma^4} \right] \right\} \right.$$

$$+ \left\{ 1 + \frac{\nu^2}{\eta^4 s^4} \left[h^2(s)h^2(\eta s) - \frac{h^2(\gamma s)h^2(\eta\gamma s)}{\gamma^4} \right] \right\} (e^{-2\epsilon} + e^{-2\delta})$$

$$\left. + \frac{\eta^2\nu^2}{\eta^4\gamma^3 s^4} h(s)h(\gamma s)h(\eta s)h(\eta\gamma s)\, e^{-\epsilon} e^{-\delta} \right) \tag{28}$$

or, retaining only powers up to s^{-4}, into

$$\Delta^{-1} \cong -\frac{4h(s)h(\gamma s)h(\eta s)h(\eta\gamma s)}{e^{\epsilon}\, e^{\epsilon}\, \eta^{8}} \left\{1 + \frac{\nu^2}{\eta^4 s^4}\left[h^2(s)h^2(\eta s) - \frac{h^2(\gamma s)h^2(\eta\gamma s)}{\gamma^4}\right]\right\}$$

$$\times\left(1 + \left\{1 + \frac{2\nu^2}{\eta^4 s^4}\left[h^2(s)h^2(\eta s) + \frac{h^2(\gamma s)h^2(\eta\gamma s)}{\gamma^4}\right]\right\}(e^{-2\epsilon} + e^{-2\delta})\right.$$

$$\left. + \frac{\eta 2\nu^2}{\eta^4\gamma^2 s^4}\, h(s)h(\gamma s)h(\eta s)h(\eta\gamma s)\, e^{-\epsilon}\, e^{-\delta}\right) \tag{29}$$

Using equations (26) and (29) in (25), one gets

$$\tilde{\tilde{u}} \cong -4h(s)h(\gamma s)\frac{f(\nu, s)r_1}{\eta^2\mu}\,\frac{e^{-\epsilon}\, e^{-\delta}}{\gamma s}\left(1 - \frac{2\nu^2}{\gamma^2\eta^2 s^2}\right)$$

$$\times\left\{1 + \frac{4\nu^2}{s^4\eta^4}\left[h^2(s)h^2(\eta s)\right] + \frac{h^2(\gamma s)h^2(\eta\gamma s)}{\gamma^4}\right\}$$

$$\times\left[\sinh\delta - \frac{4\nu^2}{\eta^4\gamma^2 s^4}\, h(s)h(\gamma s)h(\eta s)h(\eta\gamma s)\right]$$

$$\times\left(1 + \left\{1 + \frac{2\nu^2}{\eta^4 s^4}\left[h^2(s)h^2(\eta s) + \frac{h^2(\gamma s) + h^2(\eta\gamma s)}{\gamma^4}\right]\right\}(e^{-2\epsilon} + e^{-2\delta})\right.$$

$$\left. + \frac{\eta 2\nu^2}{\eta^4\gamma^2 s^4}\, h(s)h(\gamma s)h(\eta s)h(\eta\gamma s)\, e^{-\epsilon}\, e^{-\delta} + \cdots\right) \tag{30}$$

where, for repetition,

$$f(\nu, s) = \frac{2\pi p_0}{s}\, e^{-s/v}\, \frac{e^{g(|\nu|, s/v)}}{h(s/v)} \tag{31}$$

In order to invert equation (30) with respect to θ, one takes the inverse Fourier transform

$$\bar{u} = \frac{1}{2\pi} \int_{-\infty}^{\infty} \tilde{\bar{u}}(\nu, s)\, e^{-i\nu\theta}\, d\nu \tag{32}$$

This means that integrals of the form

$$I = \int_{-\infty}^{\infty} p(h)\nu^{k}\, e^{-\epsilon + g(|\nu|, s/v) - i\nu\theta}\, d\nu \tag{33}$$

must be evaluated for large values of s. p(h) represents the polynominals in the various h functions. The integrals are evaluated by finding the saddle points of

$$-\epsilon(\nu, s) + g(|\nu|, s/v) - i\nu\theta \tag{34}$$

However, in the present case, interest is centered only on the point $\theta = 0$. This simplifies matters considerably. Further, the h function cannot be simplified until the appropriate saddle point paths are determined.

Some general considerations can be inferred from equation (30), before inversion. The quantity ϵ is associated with dilatational effects as can be seen by putting ϵ in a dimensional form; similarly, δ is concerned with equivoluminar effects. In order to arrive at equation (29), a series of terms with higher powers of $e^{-\epsilon}$ and $e^{-\delta}$ is terminated with the term $(e^{-2\epsilon} + e^{-2\delta})$ and $e^{-\epsilon} e^{-\delta}$. These terms represent reverberations. Further, in equation (30) the terms $e^{-\epsilon}$ and $e^{-\delta}$ represent the time delay necessary for the P and

S waves to reach the back face. This becomes clearer as the analysis proceeds. For simplicity, only the first reverberations are considered and the terms containing $e^{-\epsilon}$ $e^{-\delta}$, etc., are dropped. It is obvious how to treat them. Since we are only interested in $\dot{u}$ directly behind the pressure front, only the case of $\theta = 0$ will be treated. For other values of θ, the saddle path becomes much more complicated.

III. INVERSION

From the above remarks, one can see that during the first reverberation

$$\tilde{\dot{u}} = -4 \frac{f(\nu, s) r_1}{\eta^2 \mu} \frac{h(s)h(\gamma s)}{\gamma s} \left\{ 1 + \frac{4\nu^2}{s^4 \eta^4} \left[(h^2(s)h^2(\eta s) + \frac{h^2(\gamma s)h^2(\eta \gamma s)}{\gamma^4} \right] \right\}$$

$$\times \left[e^{\delta} - \frac{4\nu^2}{\eta^4 \gamma^2 s^4} h(s)h(\gamma s)h(\eta s)h(\eta \gamma s)\, e^{\epsilon} \right] e^{-\epsilon}\, e^{-\delta} \tag{35}$$

where $f(\nu, s)$ is given by equation (31).

Thus, integrals of the form

$$I = \int_{-\infty}^{\infty} p(h) \nu^k e^{-s/v - \epsilon + g(|\nu|, s/v)} d\nu \tag{36}$$

where $p(h)$ is a polynomial function of h, must be evaluated. First consider ϵ, which, from equation (27.2), increases monotonically with ν. Next consider

$$g\left[|\nu|, \left(\frac{s}{v}\right)\right] - \frac{s}{v}$$

This function starts out at $\nu = 0$. Since $g(\nu, x)$ is monotone, decreasing with ν, then $g(\nu, s/\nu) - s/\nu$ is always negative. Thus, the argument of the

exponential in equation (36) is maximum at $\nu = 0$. A simple expansion shows it has a saddle point at $\nu = 0$. After some algebra, one has, for $s \gg \nu$,

$$\delta - g\left[\nu, \left(\frac{s}{v}\right)\right] + \frac{s}{v} = \eta s(1 - \gamma) + \frac{\nu^2}{2s}\left[\frac{1}{\eta}\left(\frac{1}{\gamma} - 1\right) + v\right] \tag{37}$$

$$\epsilon - g\left[\nu, \left(\frac{s}{v}\right)\right] + \frac{s}{v} = s(1 - \gamma) + \frac{\nu^2}{2s}\left[\left(\frac{1}{\gamma} - 1\right) + v\right] \tag{38}$$

The second terms in equations (37) and (38) are positive so that $\nu = 0$ is always a saddle point. Since the saddle point is at $\nu = 0$, the $h(\nu, s)$ functions must be expanded around $\nu = 0$ for large values of s. By expanding and collecting terms, one gets

$$\begin{aligned}\tilde{\dot{u}} = {} & \frac{4r_1}{\lambda + 2\mu} p_c (2\pi)^{1/2} \frac{(\eta)^{1/2}}{(s)^{1/2}} \\ & \times \left[1 + \frac{\nu^2}{s}\left(\frac{4}{\eta^2} - \frac{2}{\eta^2\gamma^2} + \frac{1}{4}\right)\left(1 + \frac{1}{\gamma^2} - v^2\right)\right] e^{-\epsilon + g(s/v) - s/v} \\ & - \frac{4\nu^2}{\eta^2\gamma s^2} e^{-\delta + g(s/v) - s/v}\end{aligned} \tag{39}$$

In equation (39) terms of order less than $1/s^2$ are dropped. Equation (39) is now multiplied by $d\nu/2\pi$ and integrated from $-\infty$ to $+\infty$. This yields the velocity at $\theta = 0$. The result is

$$\bar{\dot{u}} = \frac{-4r_1 p_o}{\lambda + 2\mu} \frac{1}{s} \frac{(\gamma v)^{1/2}}{[(1/\gamma - 1) + v]^{1/2}}$$

$$\times \left\{ \left[1 + \frac{1}{s} \frac{4/\eta^2 - 2/\gamma^2\eta^2 + 1/4 + 1/4\gamma^2 - v^2/4}{(1/\gamma - 1) + v} \right] \right.$$

$$\times e^{-s(1-\gamma)} - \frac{1}{s} \frac{4}{\eta^2\gamma}$$

$$\left. \times \frac{[(1/\gamma - 1) + v]^{1/2}}{[1/\eta(1/\gamma - 1) + v]^{3/2}} e^{-s\eta(1-\gamma)} \right\} \tag{40}$$

Now, $e^{-(1-\gamma)s}$, in nondimensional terms, represents the time delay necessary for a P wave to travel across the specimen. Similarly, $e^{\eta(1-\gamma)s}$ represents the time for the S wave to traverse the specimen. With these times denoted by t_p and t_s, respectively. Then, equation (40) inverts to give

$$\dot{u} = \frac{-4r_1 p_o}{(\lambda + 2\mu)} \frac{(\gamma v)^{1/2}}{(1/\gamma - 1)} \left\{ \left[1 - (t - t_p)k_1 \right] H(t - t_p) - (t - t_s)k_2 H(t - t_s) \right\} \tag{41}$$

where

$$k_1 = \left[\frac{2}{\eta^2} \left(2 - \frac{1}{\gamma^2} \right) + \frac{1}{4} \left(1 + \frac{1}{\gamma^2} - v^2 \right) \right] \left[\left(\frac{1}{\gamma} - 1 \right) + v \right]^{-1}$$

$$k_2 = \frac{4}{\eta^2\gamma} \frac{(1/\gamma - 1) + v}{[1/\eta(1/\gamma - 1) + v]^{3/2}} \tag{42}$$

It is thus seen that the predicted response, equation (41), has the same form as that shown in Fig. 2; namely, a step function followed by a ramp associated with the P wave, and then followed by a downward ramp associated with the S wave. An interesting feature of the P wave ramp is that it is possible for it to be negative or downward. If v^2 can be neglected ($v \cong 0.1$ in most practical cases), then, for an upward ramp to occur,

$$\gamma^2 > \frac{2/\eta^2 - 1/4}{4/\eta^2 + 1/4} = \frac{3 - 7\nu}{9 - 15\nu} \tag{43}$$

where ν in this instance is Poisson's ratio. The physical meaning of this is not clear. The negative slope for low values of γ could imply that a spreading out process of P waves is occurring. The possibility also exists that the approximation is poor in this region. It is more likely that a downward slope is due to the spreading out process. It is worth recalling that $\gamma \cong 1$ corresponds to a thin ring, while $\gamma \cong 0$ corresponds to a thick cylinder.

During the next reverberation, additional terms due to the neglected powers of $e^{-\epsilon}$, $e^{-\delta}$, and $e^{-2\epsilon} + e^{-2\delta}$ enter in. Qualitatively speaking, these result in steeper slopes and additional delays. The actual analysis is not gone into here, but experimental results bear this out (Fig. 4).

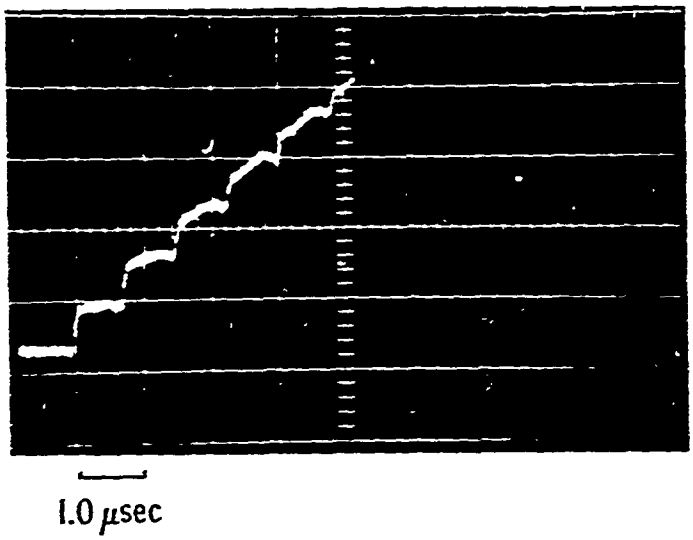

Fig. 4. Multiple Reverberation Trace

IV. NUMERICAL RESULTS AND CONCLUSIONS

Since this paper is concerned with the results of a particular experiment only that case was treated in the numerical studies. A parametric study was not carried out.

The specimen was made of aluminum, with an inner radius of 4.0 in. and a thickness of 0.40 in. It was 2 in. in the axial direction and 2 in. across in the circular direction. The material properties were taken from handbooks as well as inferred from the oscilloscope traces. The results follow:

$$E = 10.4 \times 10^6 \text{ psi}$$

$$\nu = 0.33$$

$$\mu = 3.90 \times 10^6 \text{ psi}$$

$$w = 0.101 \text{ lb/in.}^3$$

$$c_p = 2.45 \times 10^5 \text{ in./sec}$$

$$c_s = 1.22 \times 10^5 \text{ in./sec}$$

The maximum rise above the initial discontinuous jump is the quantity of greatest interest and occurs at $t = t_s - t_p$. It is calculated from equations (41) and (42) to be a 24.42 percent rise. Although numerical values taken from oscilloscope traces are difficult to obtain accurately, a sample of four gives values of 20.7, 20.5, 21.6, and 22.9 percent. This is an excellent

Preceding page blank

REFERENCES

1. Whittier, J. S., and Peck, J. C., "Experiments on Dispersive Pulse Propagation in Laminated Composites and Comparison with Theory," Journal of Applied Mechanics, Vol. 36, September 1969, p. 485.
2. Bleich, H. H. and Mindlin, R. D., Journal of Applied Mechanics, Vol. 20, 1953, p. 485.
3. Payton, R. G., "Transient Interaction of an Acoustic Wave with a Circular Cylindrical Elastic Shell," Journal of the Acoustical Society of America, Vol. 32, June 1960, p. 6.
4. Friedlander, F. G., "Diffraction of Pulses by a Circular Cylinder," Communications of Pure and Applied Mathematics, Vol. VII, 1954.
5. Miklowitz, J., "Scattering of a Plane Elastic Compressional Pulse by a Cylindrical Cavity," Proceedings of the Eleventh International Congress of Applied Mechanics, Munich, 1964.
6. Peck, J. C., and Miklowitz, J., "Diffraction of a Plane Compressional Pulse by a Circular Cavity," Proceedings on the Fifth U. S. Mathematical Congress of Applied Mechanics, Minneapolis, Minn., June 1966.
7. Carslaw, M. C. and Jaeger, Operational Methods in Applied Mathematics, Dover Press, New York, 1963.
8. Olver, F. W. "The Asymptotic Solution of Linear Differential Equations of the Second Order for Large Values of a Parameter," Philosophical Transactions of the Royal Society of London, Series A, Vol. 247, 1954.

9. Olver, F. W. J., "The Asymptotic Expansion of Bessel Functions of Larger Order," Philosophical Transactions of the Royal Society of London, Vol. 24, 1954.

10. Erde'ly et al., Higher Transcendental Functions, McGraw-Hill, New York, 1953.